

# Thermally Switched Release from Nanoparticle Colloidosomes

Shaobing Zhou,\* Jing Fan, Sujit S. Datta, Ming Guo, Xing Guo, and David A. Weitz\*

Nanoparticle colloidosomes, whose release can be switched on and off in response to a temperature change, are fabricated. Unlike in other systems, the switchable release does not require the colloidosome shell to deform; it instead occurs due to the adsorption or desorption of a block copolymer, dissolved in the core, at the inner surface of the colloidosome shell, concomitantly blocking or unblocking the pores in the shell. The colloidosomes are prepared using double emulsion templates produced by microfluidics, and are thus highly monodisperse; moreover, they are mechanically stable and consist of biocompatible components, making them suitable for the encapsulation, delivery, and release of a broad range of active materials.

## 1. Introduction

Microcapsules consisting of a shell of densely-packed colloidal particles are known as colloidosomes. They are promising candidates for the encapsulation and release of many technologically important active materials, including pharmaceuticals, cosmetics, and food preservatives.<sup>[1–3]</sup> These applications often require the microcapsules to fully encapsulate the active material, releasing it only when exposed to an external stimulus, such as a change in temperature, pH, or salt concentration. However, due to the large pores formed by the interstices between the particles, colloidosomes are inherently leaky;<sup>[4]</sup> when the encapsulated active is sufficiently small, it diffuses through these pores and is spontaneously released.<sup>[5,6]</sup> Consequently, unless the permeability of the shell, which is determined by the morphology of the pores, can be precisely controlled, colloidosomes cannot be used for applications requiring effective encapsulation and controlled release. The requisite control of the pore morphology can be achieved by fabricating colloidosomes with microgel polymers cross-linked throughout their interiors,<sup>[6]</sup> or with shells comprised of small microgel particles;<sup>[7,8]</sup> in both of these cases,

the microgels shrink or swell in response to an external stimulus, changing the size of the pores in the shell, and therefore the ability of an encapsulated material to be released. This approach has serious limitations, however. For example, the swelling or shrinking of the deformable microgels can induce undesirable, often irreversible, mechanical instabilities of the colloidosome shell. Moreover, the polymerization process to form microgels often requires harsh processing conditions, such as the use of toxic chemicals, UV-light exposure, or high reaction temperatures; these may degrade or even completely destroy the

encapsulated actives. Thus, alternative approaches to control the pore morphology are essential if colloidosomes are to be widely adapted for this class of encapsulation.

In this paper, we present a straightforward approach to make monodisperse colloidosomes that fully encapsulate an active material, only releasing it in response to an external stimulus. Here, we choose a temperature change for the stimulus, as this is one of the most commonly encountered needs. We dissolve a thermo-sensitive triblock copolymer in the aqueous colloidosome cores. Under ambient conditions, this polymer adsorbs to the surfaces of the colloidal particles making up the colloidosome shells, blocking the pores between them and fully encapsulating an active material inside the colloidosomes. However, at sufficiently high temperatures, the polymer desorbs from the particle surfaces, forming aggregates that instead remain dispersed within the colloidosome cores. This opens the pores, enabling the encapsulated active to be released through them. Importantly, this process is reversible, proceeding or becoming arrested on demand through temperature; moreover, it does not require mechanical deformations of the colloidosome shell. Our approach thus yields uniform, mechanically stable, colloidosomes with effective encapsulation and reversible temperature-controlled release. The colloidosomes consist of biocompatible components, and thus, our work describes an approach to fabricating colloidosomes that could potentially avoid toxicity issues.

## 2. Results and Discussion

### 2.1. Generation Of Double Emulsion Drops

To fabricate monodisperse colloidosomes, we produce water-in-oil-in-water (W/O/W) double emulsion drops as templates using a glass capillary microfluidic device.<sup>[9]</sup> The inner water

Prof. S. Zhou, X. Guo  
Key Laboratory of Advanced Technologies of Materials  
Ministry of Education  
School of Materials Science and Engineering  
Southwest Jiaotong University  
Chengdu, 610031, P. R. China  
E-mail: shaobingzhou@hotmail.com

Dr. J. Fan, S. S. Datta, M. Guo, Prof. D. A. Weitz  
School of Engineering and Applied Sciences  
and Department of Physics  
Harvard University  
Cambridge MA 02138, USA  
E-mail: weitz@seas.harvard.edu



DOI: 10.1002/adfm.201301030

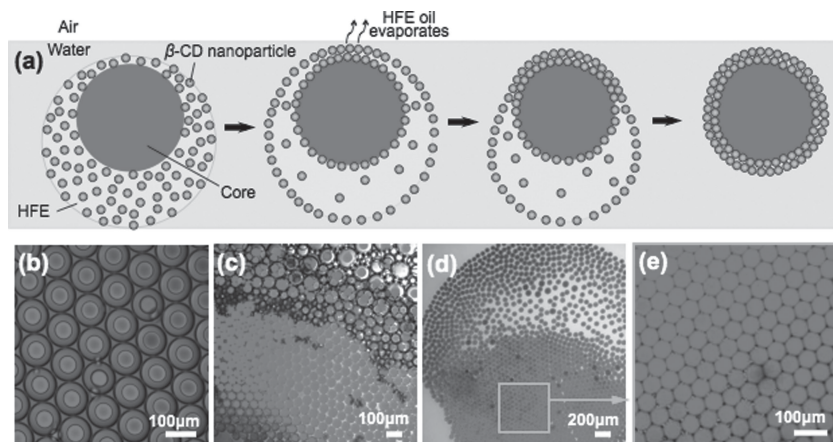


**Figure 1.** a) Side-view schematic of the dewetting transition from a double emulsion drop to a colloidosome; b–e) dewetting transition to form nanoparticle colloidosomes observed with a confocal microscope: b) monodisperse double emulsion drops with fluorescently-dyed cores, c,d) a large number of colloidosomes during dewetting, and e) closely packed monodisperse colloidosomes. Image in (b) is obtained after double emulsions are formed, while images in (c) and (d) are obtained after evaporation of the continuous aqueous phase, several minutes after the double emulsion suspension is exposed to air.

phase is a 6 wt% aqueous solution of Pluronic L31, a triblock copolymer ( $M_w \approx 1100$ , radius of gyration  $\approx 0.71$  nm; Sigma-Aldrich), with sulforhodamine B ( $M_w = 580.66$ ; Sigma-Aldrich), a red dye, at a concentration of 2 mM for subsequent characterization of the release.

The middle oil phase is a fluorinated oil HFE 7500 (3M), containing  $\beta$ -cyclodextrin ( $\beta$ -CD) nanoparticles to form the colloidosome shell, and 1 wt% Krytox-PEG surfactant to stabilize the double emulsion drops from coalescing.<sup>[10]</sup> We obtain the  $\beta$ -CD in powder form (Sigma-Aldrich); prior to its use, we dissolve it in dimethylformamide (DMF) and graft acrylic acid onto it by esterification, increasing the carbonyl content of the  $\beta$ -CD molecules. We then precipitate the modified  $\beta$ -CD in acetone, dry it, re-suspend it in DMF at a concentration of 66.6 mg/mL, and then gently mix the resultant solution into HFE 7500 oil containing 1 wt% Krytox-PEG surfactant at a volume ratio of 15% DMF solution to 85% HFE oil. This protocol forces the  $\beta$ -CD to precipitate, forming nanoparticles which remain stably suspended in the HFE 7500. After leaving the mixture to rest for 12 h, we remove the DMF floating on top of the HFE 7500 and filter the remaining HFE 7500 solution with a 250 nm-pore syringe filter. This leaves spherical, 10–30 nm diameter  $\beta$ -CD nanoparticles in the solution, as verified by the transmission electron microscopy image shown in Figure S1, Supporting Information. We use this HFE solution as the middle oil phase of the double emulsion drops.

The outer phase is a 10 wt% aqueous solution of poly(vinyl alcohol) (PVA,  $M_w$  13000–23000, 87–89% hydrolyzed; Sigma-Aldrich). By adjusting the flow rates of the three phases, we obtain monodisperse double emulsion drops, each containing a single drop in the core, as shown in Movie S1, Supporting Information. To maintain their integrity, we collect the double emulsion drops in a 3 wt% aqueous solution of poly(ethylene glycol) (PEG,  $M_w$  6000; Sigma-Aldrich) with 35 mM sodium chloride; the osmolarity of this solution is  $95 \pm 2$  mOsm  $L^{-1}$ , comparable to that of the inner and outer phases, thus preventing the

buildup of an osmotic pressure difference across the middle phase of the double emulsion. The nanoparticles adsorb to the interfaces between the inner and middle phases and the middle and outer phases, thereby reducing the interfacial energy;<sup>[11]</sup> moreover, the nanoparticles bind strongly to each other through hydrogen bonds. As a result, the double emulsion drops are highly stable, and robustly encapsulate an active material; indeed, we observe no release of the red dye from the inner phase over an observation period of six months.

## 2.2. Transition from Double Emulsions To Colloidosomes

To fabricate monodisperse colloidosomes, we expose the suspension of double emulsion drops to the ambient environment; this causes the continuous aqueous phase, and eventually, the middle oil phase, to evaporate.

The inner phase is less dense than the middle phase; thus, the innermost drop rises under gravity, causing the middle phase to be thinnest at the top of each double emulsion drop.<sup>[12]</sup> This inhomogeneity nucleates the dewetting of the oil as it evaporates, schematically illustrated in Figure 1a.<sup>[13]</sup> After the continuous aqueous phase evaporates, the oil quickly detaches from the inner drop in less than 0.1 s (Movie S2, Supporting Information), over an order of magnitude faster than dewetting in other systems;<sup>[14]</sup> this behavior reflects the combined effects of the inhomogeneity of the double emulsion middle phase and the strong attractive interactions between the nanoparticles coating the surfaces of the middle phase. The dewetting leaves the colloidosomes armored with layers of densely packed nanoparticles, producing a large number of colloidosomes within just a few seconds, as shown in Figure 1b–d. To prevent them from drying and deforming, we add distilled water to the colloidosomes within 1–2 min, and subsequently add an aqueous solution of 20 vol% isopropanol to remove any residual HFE oil from the shell. We then replace the isopropanol in the continuous phase with distilled water. The resultant colloidosomes are approximately 50  $\mu$ m in diameter, and are highly monodisperse; this is reflected by their precise hexagonal packing structure, shown in Figure 1e. The colloidosome shells are only  $\approx 40$  nm thick, consisting of 2–3 densely-packed nanoparticle layers, as shown by the freeze-fracture cryo-scanning electron microscope (cryo-SEM) images in Figure 2.

## 2.3. Reversible, Thermo-Sensitive Release

The pores formed in the interstices between the nanoparticles are roughly 1.5–4.5 nm in diameter;<sup>[1]</sup> unfortunately, this is sufficiently large for small and medium-sized molecules to diffuse through and become spontaneously released from the colloidosomes. We overcome this problem by dissolving the L31 copolymer in the colloidosome cores; the temperature-sensitive

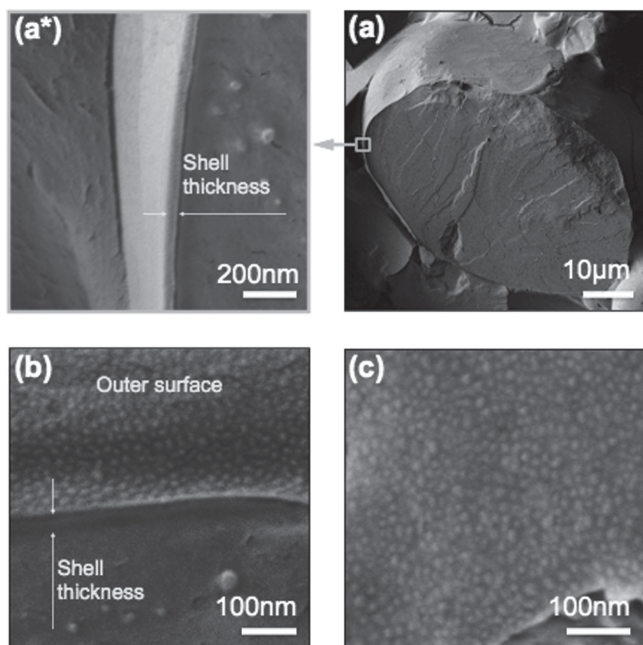


**Figure 2.** Freeze-fracture cryo-scanning electron microscope (cryo-SEM) images of the colloidosome: a) a fractured colloidosome with a highly magnified view of the region in blue shown in panel (a\*), b) the cross-section and outer surface of a thin shell, and c) the outer surface of the shell consisted of densely packed nanoparticles.

phase behavior of this copolymer provides a straightforward means to control the colloidosome pore morphology, and thus, the encapsulation and release characteristics. We quantify this behavior by monitoring the change in the fluorescence intensity of the colloidosome cores, containing a small encapsulated dye, of two different samples, with distilled water as the continuous phase, over time. One sample is stored at 37 °C for 19 days. Similar to measurements on typical colloidosome systems, the measured fluorescence intensity for this sample decreases over the entire observation period, indicating that the encapsulated dye is continually released from the colloidosome cores (black squares in Figure 3). We also store the second sample at 37 °C, but only for 4 days; during this period, the fluorescence intensity similarly decreases, indicating that the encapsulated dye is released (red circles with solid connectors in Figure 3). We then store this sample at 21 °C for 11 days; strikingly, in stark contrast to the case of the first sample, we observe that the fluorescence intensity remains constant over this time period (red circles with dashed connectors in Figure 3). This shows that a reduction in temperature arrests the release from the colloidosome cores. To subsequently re-trigger the release, we again store the sample at 37 °C for 4 days. We observe a concomitant decrease in the fluorescence intensity (red circles with solid connectors in Figure 3), indicating that the encapsulated dye is released once again, and confirming that the triggered release is fully reversible.

The thermosensitive release results from the unique phase behavior of the L31 copolymer.<sup>[15]</sup> To elucidate this behavior, we prepare a bulk aqueous solution of 6 wt% L31 copolymer

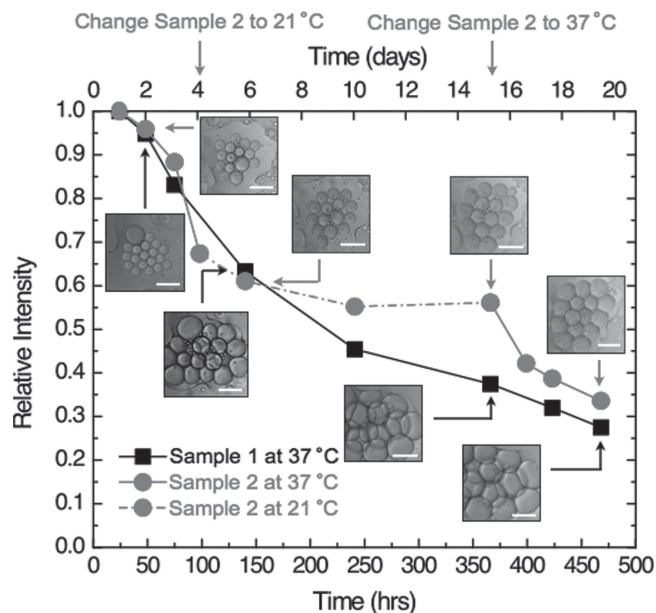


**Figure 3.** Attenuation of the fluorescence intensity in the two samples, each consisting of multiple colloidosomes, at different temperatures, measured using confocal microscopy. The insets are combinations of the fluorescence and bright-field images, in which the scale bars are 200 μm.

containing sulforhodamine B for visualization. At 21 °C, the solution is completely transparent, as shown in Figure 4a, indicating that the copolymer is dispersed as individual molecules. We hypothesize that this enables the hydroxyl groups of the copolymer molecules to hydrogen bond to the carbonyl groups of the nanoparticles making up the colloidosome shells;<sup>[15]</sup> consequently, the L31 copolymer preferentially adsorbs to the nanoparticle surfaces. The L31 radius of gyration is  $\approx 0.71$  nm,<sup>[16]</sup> close to the size of the interstitial pores of the colloidosome shells; we thus expect that the L31 adsorption blocks, and prevents release of an active material through, the pores, as schematized in Figure 4d, consistent with the experimentally observed encapsulation behavior. By contrast, when heated to 37 °C, the copolymer solution becomes opaque, as shown in Figure 4b; direct visualization by confocal microscopy reveals that this is due to the formation of 1 μm L31 copolymer aggregates, shown in Figure 4c. This observation indicates that, at this elevated temperature, the associations between the hydrophobic PPO groups of the copolymer molecules dominate the L31 phase behavior.<sup>[17]</sup> We thus expect that the copolymer molecules desorb from the nanoparticle surfaces, instead forming aggregates that remain dispersed within the colloidosome cores, as schematized in Figure 4e. This opens the pores in the colloidosome shells, enabling the release of the encapsulated active through them, consistent with the experimentally observed release. Importantly, we find that the formation of the copolymer aggregates at this high temperature, and their breakup into individual molecules under ambient conditions, is completely reversible; as a result, we expect the triggered release to be fully reversible, in complete agreement with our experimental observations. Because the phase behavior of the

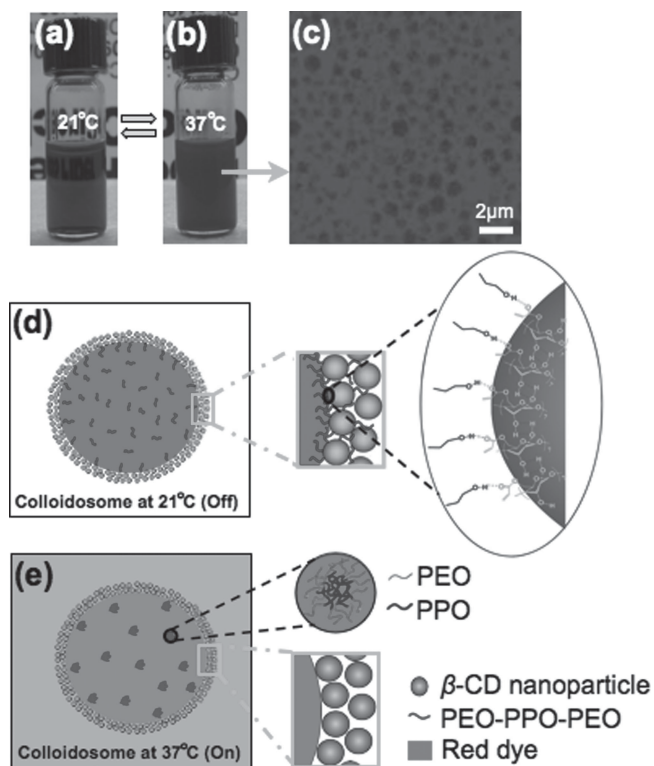


**Figure 4.** a–c) Temperature responsivity of the aqueous solution of 6.0 wt% Pluronic L31 copolymer with the 2.0 mM of red sulfurodamine B dye. The solution alternates between a) transparent and b) opaque as the temperature varies between 21 °C and 37 °C; c) confocal microscope image of the solution at 37 °C, showing L31 aggregates. d–e) Schematic of the thermally-switched release: d) at 21 °C, PEO–PPO–PEO copolymers block the interstitial pores in the shell, switching off the release and enabling effective encapsulation (PEO: polyethylene glycol; PPO: Poly(p-phenylene oxide)); e) at 37 °C, PEO–PPO–PEO copolymers aggregate, opening the interstices and switching on the release from the colloidosome core.

L31 copolymer is sensitive to the concentration used, we anticipate that the L31 concentration may provide a means to tune the temperature triggering the release.

#### 2.4. Colloidosome Mechanical Stability

To be applied for the encapsulation, delivery, and release of active materials, colloidosomes must be robust against extreme deformations. We probe the mechanical stability of our colloidosomes, with distilled water as the continuous phase, by monitoring their morphological evolution using optical microscopy. The copolymer and dye molecules in the colloidosome cores exert a strong osmotic pressure on the colloidosome shells; this forces them to swell over the course of the release experiments to more than twice their original size, as shown by the optical image insets to Figure 3. Interestingly, we observe that the rate at which the colloidosomes swell is dramatically reduced at 21 °C, compared to at 37 °C; this further reflects the blockage of the pores in the colloidosome shells, preventing the transport of both water and dye through the shell, under ambient

conditions.<sup>[18]</sup> The maximal colloidosome swelling corresponds to a shell strain of over 100%; remarkably, even under these extreme mechanical deformations, the colloidosomes remain fully intact. This enhanced mechanical stability highlights the suitability of our experimental system for the encapsulation, delivery, and release of a broad range of active materials.

### 3. Conclusions

In summary, we present an approach to thermally switch release from nanoparticle colloidosomes. We fabricate monodisperse, mechanically stable colloidosomes. While the entire fabrication process used here may not be biocompatible, both the  $\beta$ -CD nanoparticles and the L31 copolymers comprising the colloidosomes are. Thus, our work suggests a promising route to potentially avoid toxicity issues, and could enable the production of colloidosomes that are suitable for the encapsulation, delivery, and release of active materials in a wide variety of situations in the food, pharmacology, and cosmetics industries. The approach described here is general, and can be modified for specific applications; for example, the release rate from the colloidosome core, or the stimulus triggering the release, can be varied by varying the size of the nanoparticles making up the colloidosome shell or by employing different types of copolymers that are responsive to various environmental stimuli such as pH, light, glucose concentration, or a change in oxidation state.

### Supporting Information

Supporting Information is available from the Wiley Online Library or from the author.

### Acknowledgements

S.Z. and J.F. contributed equally to this work. This work was partially supported by the National Basic Research Program of China (973 Program, 2012CB933600), National Natural Science Foundation of China (numbers 30970723 and 51173150), the NSF (DMR-1006546), and the Harvard MRSEC (DMR-0820484). The authors thank R. Sperling for synthesizing the surfactant, A. Ehrlicher and L. Jawerth for assistance with laser scanning confocal microscopy, and the anonymous reviewers for useful comments. J.F. thanks N. Antoniou for his assistance in cryo-SEM. S.S.D. acknowledges funding from ConocoPhillips.

Received: March 25, 2013

Revised: April 25, 2013

Published online: June 26, 2013

- [1] A. D. Dinsmore, M. F. Hsu, M. G. Nikolaidis, M. Marquez, A. R. Bausch, D. A. Weitz *Science* **2002**, *298*, 1006.
- [2] M. F. Hsu, M. G. Nikolaidis, A. D. Dinsmore, A. R. Bausch, V. D. Gordon, X. Chen, J. W. Hutchinson, D. A. Weitz *Langmuir* **2005**, *21*, 2963.
- [3] S. Shilpi, A. Jain, Y. Gupta, S. K. Jain *Crit. Rev. Ther. Drug Carrier Syst.* **2007**, *24*, 361.
- [4] S. S. Datta, H. C. Shum, D. A. Weitz *Langmuir* **2010**, *26*, 18612.

- [5] H. W. Duan, D. Y. Wang, N. S. Sobal, M. Giersig, D. G. Kurth, H. Mohwald *Nano Lett.* **2005**, *5*, 949.
- [6] J. W. Kim, A. Fernandez-Nieves, N. Dan, A. S. Utada, M. Marquez, D. A. Weitz *Nano Lett.* **2007**, *7*, 2876.
- [7] D. B. Lawrence, T. Cai, Z. B. Hu, M. Marquez, A. D. Dinsmore *Langmuir* **2007**, *23*, 395.
- [8] R. K. Shah, J. W. Kim, D. A. Weitz *Langmuir* **2009**, *26*, 1561.
- [9] A. S. Utada, E. Lorenceau, D. R. Link, P. D. Kaplan, H. A. Stone, D. A. Weitz *Science* **2005**, *308*, 537.
- [10] C. Holtze, A. C. Rowat, J. J. Agresti, J. B. Hutchison, F. E. Angile, C. H. J. Schmitz, S. Koster, H. Duan, K. J. Humphry, R. A. Scanga, J. S. Johnson, D. Pisignano, D. A. Weitz *Lab Chip* **2008**, *8*, 1632.
- [11] S. Levine, B. D. Bowen, S. Partridge *Colloids Surf.* **1989**, *38*, 325.
- [12] S. S. Datta, S. H. Kim, J. Paulose, A. Abbaspourrad, D. R. Nelson, D. A. Weitz *Phys. Rev. Lett.* **2012**, *109*, 134302.
- [13] R. Hayward, A. S. Utada, N. Dan, D. A. Weitz *Langmuir* **2006**, *22*, 4457–4461.
- [14] H. C. Shum, E. Santanach-Carreras, J. W. Kim, A. Ehrlicher, J. Bibette, D. A. Weitz *J. Am. Chem. Soc.* **2011**, *133*, 4420.
- [15] P. Alexandridis *Curr. Opin. Colloid Interface Sci.* **1997**, *2*, 478.
- [16] S. Nawaz, M. Redhead, G. Mantovani, C. Alexander, C. Bosquillon, P. Carbone *Soft Matter* **2012**, *8*, 6744.
- [17] J. Szejtli *Chem. Rev.* **1998**, *98*, 1743.
- [18] The colloidosomes remain swollen even when the temperature is reduced to 21 °C, as shown by the optical images in Figure 3; however, the release from their cores becomes arrested at this temperature. This indicates that the phase behavior of the L31 copolymer, not the swelling of the colloidosome, causes the release from the colloidosome core.